Seasonal Variability in the Microbial Plankton Community in a Semienclosed Bay Affected by Upwelling: The Role of a Nutrient Trap

Francisco G. Figueiras[1]*, Isabel G. Teixeira[2], María Froján[1], Diana Zúñiga[1], Belén Arbones[1] and Carmen G. Castro[1]

[1] *Consejo Superior de Investigaciones Científicas, Instituto de Investigaciones Marinas, Vigo, Spain,* [2] *CESAM – Centre for Environmental and Marine Studies, Department of Biology, University of Aveiro, Aveiro, Portugal*

The Ría de Vigo is a semienclosed bay in northwestern Iberia that is affected by seasonal upwelling (spring to autumn) that triggers high levels of primary productivity. Fisheries and aquaculture coexist with other human activities, such as shipbuilding and tourism, in this area. The microbial plankton community in this system was studied to understand how this community is structured and progresses seasonally. Autotrophic biomass (AB) dominated from spring to autumn when upwelling prevailed, while AB and heterotrophic biomass (HB) covaried throughout the year as HB:AB = 0.26 ± 0.04 (r^2 = 0.7), indicating a link between the two communities. Diatoms and autotrophic nanoflagellates accounted for 80 ± 18% of the AB, whereas the HB was mainly composed of heterotrophic bacteria (36 ± 11%) and heterotrophic nanoflagellates (30 ± 12%). The AB and HB, as well as their main components, showed a continuous increase during the upwelling season that was attributed to growth. However, a sudden increase occurred in autumn, when downwelling caused the biomass to accumulate before leading to the low values in winter. As upwelling promotes the export of materials to the open ocean, the increase in biomass was possibly due to the existence of a nutrient trap that fueled phytoplankton growth through recycling at the sediment-water interface a substantial portion of the organic matter previously synthetized in the water column. The reorganization of the community that followed the winter decrease in biomass began with the proliferation of small plankton forms.

Keywords: microbial plankton biomass, seasonal increase, upwelling, nutrient trap, semienclosed bay

INTRODUCTION

Coastal seas, which represent only 7–10% of the ocean's surface, account for a large fraction (∼20–30%) of marine primary production (Wollast, 1998; Bauer et al., 2013), which is sustained by high proportions of regenerated nutrients (Billen, 1978; Boynton et al., 2018). Because of this, coastal seas are among the most valuable oceanic regions in the world, supplying significant quantities of seafood for humans through fishing and aquaculture (Holligan and de Boois, 1993;

Millennium Ecosystem Assessment, 2005). Nevertheless, these areas also support high densities of people, with approximately half of the world's population living within 60–100 km of the coastline (Cohen et al., 1997; Sale et al., 2014); as a result, coastal seas are extremely vulnerable to anthropogenic influences (Jickells, 1998; Cloern et al., 2016). Anthropogenic impacts are still higher in semienclosed bays, where water exchange with the open ocean is limited to some extent. Furthermore, these sheltered waters are the preferred location for human settlement, where fishing and aquaculture, among other human activities, thrive. As it is expected that seafood demand and anthropogenic impacts will continue increasing in the future due to population growth, mainly on coastal margins (Hinrichsen, 1994; Sale et al., 2014), knowledge of the functioning of these ecosystems is essential to facilitate their management and ensure the suitable conditions needed to preserve the services that they provide. In this regard, specific knowledge about the structure and variability in microbial plankton communities is of exceptional relevance. Primary production and the first transfers of matter and energy within the pelagic realm take place in these communities, and thus, microbial plankton bring the supporting services needed for the development of all other ecosystem services (Lubchenco and Petes, 2010).

The Rías Baixas are four semienclosed bays located on the northwestern Iberian Peninsula (**Figure 1**); mussel culture is an important socioeconomic activity in this area (Figueiras et al., 2002) that currently coexists with other urban and industrial activities that have been promoted by population increases in coastal villages and cities (Fernández et al., 2016). The region is at the northern limit of the North Atlantic upwelling ecosystem, which extends from the south of Senegal at approximately 10°N (Wooster et al., 1976). At the northwestern Iberian margin, upwelling is seasonal, with episodes of northerly winds that promote upwelling events from spring to autumn and southerly winds that trigger downwelling in winter (Wooster et al., 1976; Figueiras et al., 2002). This upwelling-downwelling regime directly affects the Rías Baixas, which act as a shelf prolongation. It forces the main circulation pattern in the Rías, which is positive (estuarine-like) during upwelling and the reverse during downwelling events (Figueiras et al., 2002; Crespo et al., 2006; Barton et al., 2015, 2016), and determines the response of the microbial plankton community (Figueiras et al., 1994; Teixeira et al., 2011; Froján et al., 2014). Strong upwelling events, through positive estuarine circulation, wash out plankton communities toward the shelf leading to a high nutrient, low biomass scenario inside the Rías and to the homogenization of the whole water column (Álvarez-Salgado et al., 2010). On the contrary, weak and moderate upwelling conditions, associated to lower transport rates and to the inability to disrupt the stratified plankton-rich surface layers (0–10 m), provide nutrients to these layers promoting high *in situ* phytoplankton growth (Figueiras et al., 1994; Piedracoba et al., 2005). Short-term upwelling-downwelling sequences result in the occurrence of harmful algal blooms (HABs) inside the Rías at the end of the upwelling season (Fraga et al., 1988; Tilstone et al., 1994; Fermín et al., 1996; Crespo et al., 2006, 2007); upwelling favors the growth of these harmful species in the outer part of the Rías and in the nearby
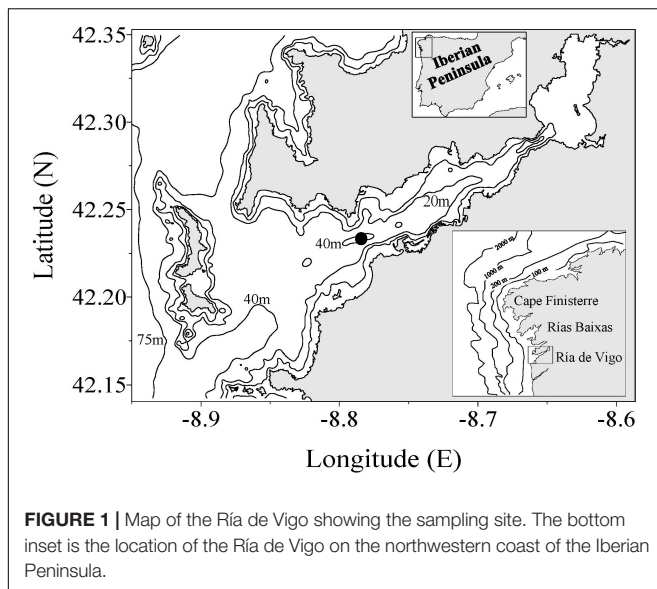
shelf, and downwelling accumulates these species in the interior. These HAB episodes interrupt the commercial extraction of mussels, causing important economic losses to this aquaculture sector (Figueiras et al., 2002). In general, environmental short-term variability influences microplankton dynamics, promoting the maintenance of functional diversity, even though seasonal succession is a main feature of microplankton populations (Nogueira et al., 2000). On the other hand, upwelling through nutrient supply is responsible for high levels of primary production (Tilstone et al., 1999; Cermeño et al., 2006; Arbones et al., 2008) that fuel mussel growth in the Rías (Blanton et al., 1987; Figueiras et al., 2002; Zúñiga et al., 2013; Froján et al., 2014). However, not all primary production is consumed in the pelagic environment; a substantial portion of photosynthesized matter sinks and is remineralized in the sediments (Alonso-Pérez and Castro, 2014), which means that the Rías are environments that trap nutrients that are initially supplied by upwelling.

Despite all this research, studies focused on characterizing the structure of the whole microbial plankton community in relation to environmental and oceanographic conditions in the Rías Baixas are limited (Teixeira et al., 2011; Froján et al., 2014), and the research has been constrained to certain seasonal periods. Surprisingly, there are no studies analyzing the entire microbial plankton community during a whole annual cycle in this coastal upwelling system. Therefore, here, we revisit data collected in the early 1990s to assess for the first time the structure of the microbial plankton community (from pico- to micro-plankton) and distinguish among autotrophs and heterotrophs in the Ría de Vigo on an annual basis (**Figure 1**). The aim was to track the seasonal variability in the microbial plankton community in response to seasonal environmental forcing in a temperate semienclosed bay of ecological interest, where fisheries and aquaculture coexist with shipbuilding and tourism (Huntington et al., 2015; Fernández et al., 2016). Specifically, we wanted to know the main components of both autotrophic and heterotrophic microbial plankton and how they progressed through the upwelling-downwelling seasons. Our interest also focused on the role played by the Ría as a nutrient trap in the development of the microbial plankton community. Due to the time elapsed since data collection, the gathered knowledge could be the baseline to which changes in the microbial plankton community induced by alterations in environmental conditions occurring in this and other similar semienclosed bays forced by upwelling can be compared.

MATERIALS AND METHODS

Sampling

A station located in the middle of the Ría de Vigo (**Figure 1**) at the central channel (45 m depth at low tide) was visited twice a week from January to December 1991. This station has regularly been used for studies on short-term and seasonal variability in the Ría de Vigo (Nogueira et al., 2000; Nogueira and Figueiras, 2005; Crespo et al., 2006). The central position of this station in the estuary allows for the detection of both continental and oceanic influences (Figueiras et al., 1994, 2002; Barton et al., 2015). The

FIGURE 1 | Map of the Ría de Vigo showing the sampling site. The bottom inset is the location of the Ría de Vigo on the northwestern coast of the Iberian Peninsula.

innermost part of the estuary shows essentially continental influences, while positions in the outermost zone mainly represent the oceanic domain.

The sampling began with a conductivity-temperature-depth (CTD) cast and continued with the collection of seawater from the surface, the bottom of the photic layer [mean depth $\pm$ the standard deviation (SD) of the 1% incident irradiance value at the surface = 12 $\pm$ 5 m] and the bottom layer of the water column (40 m) with 5 L Niskin bottles. The temperature (°C) and salinity (S) values were extracted from the CTD (SBE 25) casts, while the chlorophyll a (chl a) and nutrient concentrations as well as the microbial plankton biomass were determined from seawater samples collected from the surface and the bottom of the photic layer. The nutrient concentrations were also determined from seawater samples collected at 40 m depth. Daily determinations of incoming solar radiation, runoff and upwelling intensity complemented this sampling.

Environmental Variables

The mean incoming solar radiation (Qs) of the preceding 3 days plus the sampling day was estimated by Mosby's formula (Dietrich et al., 1980). Runoff (Qr) was calculated by the empirical equation proposed by Ríos et al. (1992) that uses a retention coefficient of 0.75 for the drainage basin (586 km^2) of the Ría de Vigo. We considered the rainfall over the preceding 3 days plus the sampling day.

The average cross-shelf ($-$Qx) and alongshore (Qy) Ekman transport for the previous 3 days plus the sampling day were estimated according to Bakun (1973) using the geostrophic winds off Cape Finisterre:

$$Q_{x.y} = -\frac{\rho_a C_d \, |V| \, V_{y,x}}{f \rho_{sw}}$$

where ρ_a is the air density at 15°C (1.22 kg m^{-3}), C_d (1.3 $\times$ 10^{-3}) is the dimensionless empirical drag coefficient, $V_{y,x}$ represents the northerly and westerly components of the

wind speed, $|V|$, over the sea surface, f is the Coriolis parameter at 43°N (9.946 $\times$ 10^{-5} s^{-1}) and ρ_{sw} is the seawater density ($\sim$1025 kg m^{-3}). The sign of Qx was changed so that positive values of $-$Qx corresponded to upwelling events.

The cross-shelf and alongshore transport calculated at Cape Finisterre are representative of the situation in the Rías Baixas (Blanton et al., 1984). Positive values of both $-$Qx and Qy correspond to upwelling, whereas negative values indicate downwelling. Positive values of $-$Qx are due to northerly winds, which induce upwelling on the shelf and promote estuarine-like circulation in the Ría. This type of circulation is characterized by the transport of surface waters from the Ría to the ocean, while upwelled water on the shelf enters the Ría through the bottom (Crespo et al., 2006). Easterly winds, however, act directly on the surface waters of the Ría, forcing their outflow toward the open ocean and thus triggering upwelling inside the Ría. In contrast, westerly winds promote the immediate intrusion of coastal surface waters into the Ría, causing downwelling (Crespo et al., 2006; Barton et al., 2015).

Nutrients and Chlorophyll

The nutrient levels were determined with a Technicon AAII autoanalyzer. The nitrate concentration was determined by reducing nitrate to nitrite in a Cd-Cu column according to the modification of Mouriño and Fraga (1985). The nitrite, phosphate and silicate concentrations were determined following Hansen and Grasshoff (1983), and the ammonia concentration was determined according to Grasshoff and Johannsen (1972).

For the chlorophyll (chl a) determination, 100 ml of seawater was filtered through 25 mm GF/F filters. The filters were then frozen at $-$20°C before the pigments were extracted in 90% acetone for 24 h at 4°C in the dark. The chl a concentrations were determined according to the methods of Yentsch and Menzel (1963) after reading the fluorescence values of the extracted pigments in a Turner Designs fluorometer that was calibrated with pure chl a (Sigma Chemical). No correction for phaeopigments was made.

Plankton Biomass

To determine the pico- and nano-plankton biomass, subsamples of 10 ml were fixed with buffered formalin (2% final concentration) and stained with DAPI at a final concentration of 0.1 µg ml^{-1} for 5 min (Porter and Feig, 1980). The samples were then filtered on 0.2 µm black Millipore polycarbonate filters placed on top of 0.45 µm Millipore backing filters. An epifluorescence microscope was used to identify and count the *Synechococcus*-type cyanobacteria (SYN), picoflagellates ($\leq$2 µm), nanoflagellates (between 2 and 20 µm) and bacteria. *Synechococcus* were identified by their yellow color, and the autotrophic pico- (APF) and nano-flagellates (ANF) were identified by their red color under excitation with blue light. The *Prochlorococcus* were not correctly identified and counted with this technique, but their presence was negligible in this coastal system (Rodríguez et al., 2003). The bacteria and heterotrophic pico- (HPF) and nano-flagellates (HNF) were counted under excitation with UV light. Some cells that are considered autotrophic under epifluorescence microscopy are actually mixotrophic (e.g., Sanders et al., 2001; Crespo et al., 2011;

Figueiras et al., 2014). The bacterial biomass was estimated according to Lee and Fuhrman (1987). For the other three groups, the cell biovolumes were converted to carbon biomass values following Bratbak and Dundas (1984) for SYN and Verity et al. (1992) for the pico- and nano-flagellates. The biovolumes were calculated after taking the dimensions of several individuals and assuming a spherical shape.

Samples preserved in Lugol's iodine and sedimented in 50 ml composite sedimentation chambers were used to identify and count the diatoms, dinoflagellates, flagellates > 20 μm and ciliates with an inverted microscope. The distinctions between autotrophic and heterotrophic species were made according to Lessard and Swift (1986) and were complemented with observations of fresh samples with an epifluorescence microscope. The biovolumes of each taxon were calculated from the dimensions and shapes according to Edler (1979). The plasmatic volume (diatoms) and total cell volume (dinoflagellates, other flagellates > 20 μm and ciliates) were converted to cell carbon values following Strathmann (1967) for diatoms and dinoflagellates, Verity et al. (1992) for flagellates and Putt and Stoecker (1989) for ciliates.

Presentation of the Results and Statistical Analysis

The inspection of the distributions of the original variables showed that the surface and bottom of the photic layer were differentiated almost exclusively by the values of plankton biomass, with higher abundance of all plankton groups in the surface waters. A companion study with the same data set (Nogueira et al., 2000) did not find significant differences in the microplankton composition between these two depths. Therefore, to simplify the presentation of the results, avoiding the "noise" caused by short-term variability in the data, only half-month averages of the results for the surface layer are shown in the figures. The number of samples used to calculate these averages varied between 3 and 5. Three samples were used in 4 averages (2 in February, 1 in March, and 1 in December) and 5 samples in 3 averages (1 in May, 1 in July, and 1 in October). Four samples were used to calculate the other 17 averages.

The half-month averages and SDs of the meteorological variables and all variables determined in the surface layer are provided as **Supplementary Tables S1–S4**. The half-month averages and SDs of the nutrient concentrations at 40 m depth can be found in the **Supplementary Table S5**. The original data set is also provided as **Supplementary Material** in an excel file (Original data. xls).

The correlation coefficients among the half-month average values of meteorological variables and the physico-chemical and biological variables determined in the surface layer are also given as **Supplementary Table S6**.

To identify the most important trends in seasonal variability in the microbial plankton community, principal component analysis (PCA) was performed on the correlation matrix among the logarithm of the half-month averaged biomasses of the microbial plankton groups in the surface layer.

RESULTS

Meteorological and Hydrographic Scenario

The incoming solar radiation (Qs, **Figure 2A**) showed the typical seasonal pattern of temperate latitudes, with low values of irradiance (125 ± 34 cal cm^{-2} d^{-1}) during winter (November to February) and the highest values (430 ± 75 cal cm^{-2} d^{-1}) in summer (June to September). The sea surface temperature progressed following solar radiation (**Figure 2A**) ($r = 0.60$, $p = 0.002$, **Supplementary Table S6**) but showed the expected delay due to heat exchanges between the atmosphere and ocean during the transition periods of spring and autumn. Thus, the

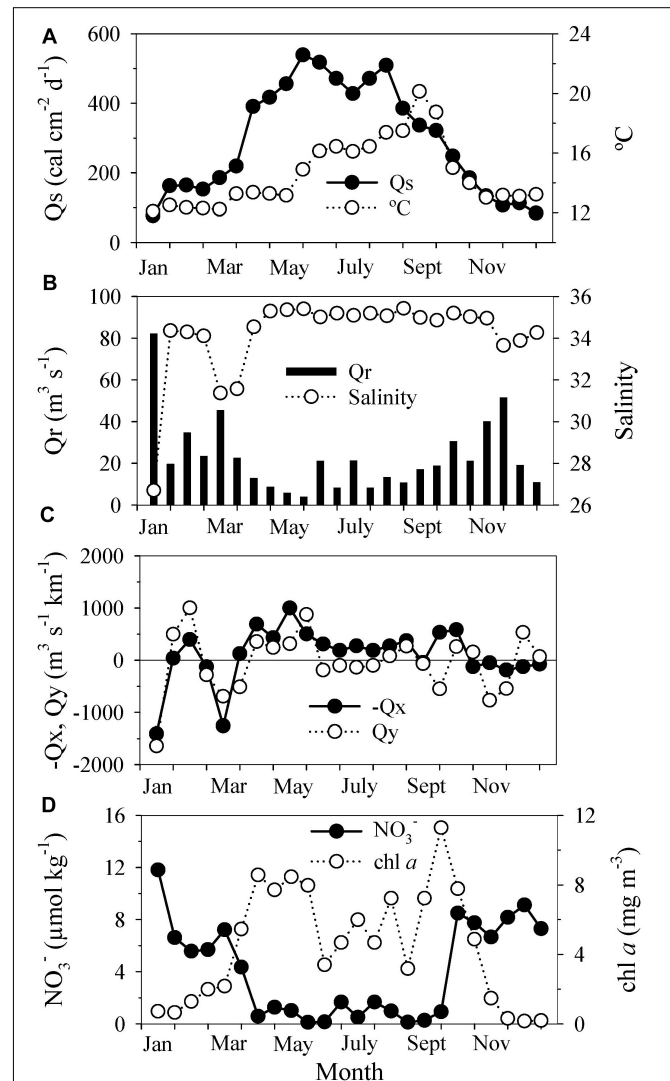**FIGURE 2 |** Time series of **(A)** incoming solar radiation (Qs) and seawater temperature (°C), **(B)** runoff (Qr) and surface salinity, **(C)** cross-shelf (–Qx) and alongshore (Qy) Ekman transport, and **(D)** nitrate (NO$_3^-$) and chlorophyll a (chl a) concentrations in the surface layer. The values were averaged every half-month ($n = 3$–5) to remove short-term variability.

highest temperature values in the surface seawater were recorded in September ($\sim20°C$), whereas those of solar radiation occurred between May and August. The seawater temperature in April remained at $\sim13°C$ when the solar radiation rose from 220 to 417 cal cm^{-2} d^{-1} (**Figure 2A**).
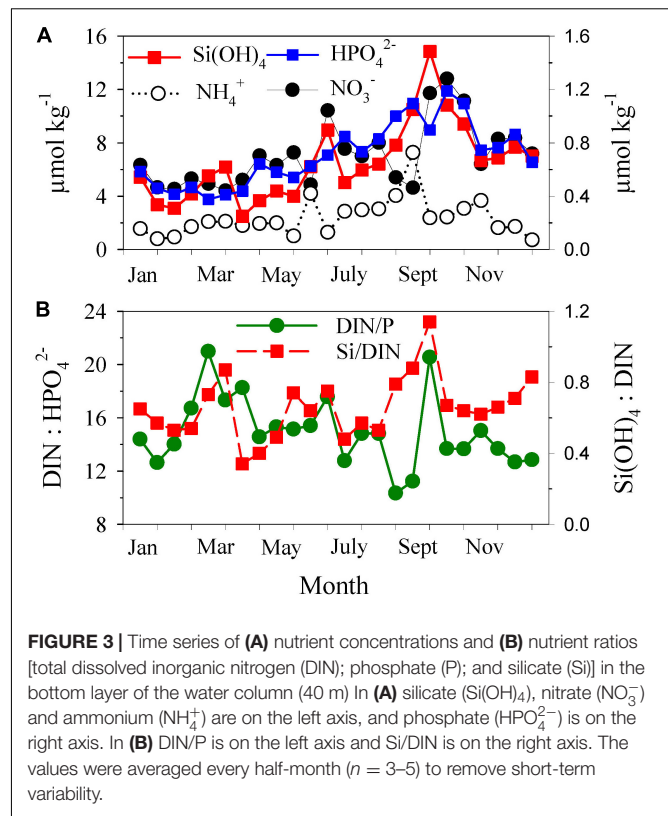
High runoff (**Figure 2B**), especially in January and March, with values above 45 m^3 s^{-1}, caused noticeable drops in salinity (**Figure 2B**) (salinity vs. runoff, $r = -0.80$, $p < 0.0001$, **Supplementary Table S6**). The highest runoff concurred with strong downwelling events (**Figure 2C**); runoff was negatively correlated with Qy and $-$Qx ($r = -0.69$, $p = 0.0002$ and -0.75, $p < 0.0001$, **Supplementary Table S6**). The downwelling episodes were more frequent and stronger during winter than during summer (**Figure 2C**), when upwelling, especially cross-shelf transport ($-$Qx), was persistent (**Figure 2C**). The transition from downwelling to upwelling occurred in March-April, while the upwelling-downwelling transition took place in September (**Figure 2C**), when the seawater temperature was highest (**Figure 2A**).

The nutrient and chl *a* concentrations (**Supplementary Table S6**), specifically the nitrate and chl *a* concentrations in the surface waters of the Ría de Vigo (**Figure 2D**), had opposite patterns (chl *a* vs. NO_3^-, $r = -0.67$, $p = 0.0003$, **Supplementary Table S6**). High nutrient concentrations in winter, which corresponded with the highest runoff (nitrate vs. runoff, $r = 0.72$, $p < 0.0001$, **Supplementary Table S6**), coincided with the lowest chl *a* values of the year (0.8 ± 0.6 mg m^{-3}). The nutrient levels were considerably lower (mean nitrate concentration $= 0.77 \pm 0.57$ μmol kg^{-1}) during the upwelling season (April to September), when the chl *a* concentration was 6.70 ± 2.4 mg m^{-3}. Within this seasonal pattern, it was possible to distinguish two maxima of chl *a*: one in spring (~8 mg m^{-3}) and the other at the end of summer (~11 mg m^{-3}). The spring maximum coincided with the first upwelling events of the year (**Figure 2C**, April–June), whereas the autumn maximum (September) was associated with the seasonal upwelling-downwelling transition (**Figure 2C**).

This time variability recorded for nutrients in the surface layer (**Figure 2D**) contrasted with that found for the nutrients in the bottom layer (**Figure 3A**), where a continuous increase in nutrient concentrations was evident from March to September. This increase occurred while the nutrient ratios DIN/P and Si/DIN did not show statistically significant trends throughout the season ($r^2 = 0.11$, $p = 0.12$ and $r^2 = 0.14$, $p = 0.08$, respectively; **Figure 3B**). Average ratios were 15 ± 3 for DIN/P and 0.7 ± 0.2 for Si/DIN.

Variability in Microbial Plankton Biomass

Both the total autotrophic (AB) and heterotrophic (HB) biomass values in the surface layer exhibited steady increases from early spring (February–March) to August (**Figure 4A**). The rate of increase in AB (23 ± 4 mg C m^{-3} per half-month) during this growth season was ~3 times higher than the increase in HB (8 ± 2 mg C m^{-3} per half-month). A sudden increase occurred in both the AB (~900 mg C m^{-3}) and HB (~300 mg C m^{-3}) in September, which was followed in October by an abrupt decrease to winter values. The AB and HB

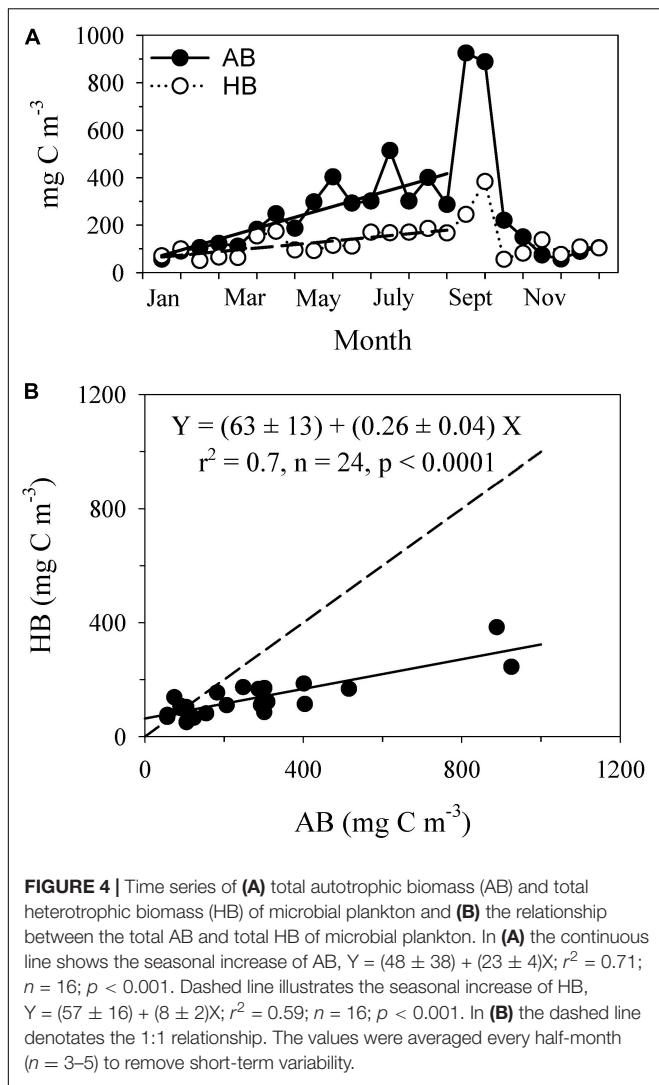**FIGURE 3 |** Time series of **(A)** nutrient concentrations and **(B)** nutrient ratios [total dissolved inorganic nitrogen (DIN); phosphate (P); and silicate (Si)] in the bottom layer of the water column (40 m) In **(A)** silicate (Si(OH)$_4$), nitrate (NO$_3^-$) and ammonium (NH$_4^+$) are on the left axis, and phosphate (HPO$_4^{2-}$) is on the right axis. In **(B)** DIN/P is on the left axis and Si/DIN is on the right axis. The values were averaged every half-month ($n = 3$–5) to remove short-term variability.

values were similar during winter (87 ± 24 and 89 ± 28 mg C m^{-3}, respectively). Nevertheless, both biomasses showed a positive linear relationship (**Figure 4B**) with a low HB:AB ratio (0.26 ± 0.04; the slope of the relationship) and a statistically significant excess in HB (63 ± 13 mg C m^{-3}; the intercept of the relationship) for a hypothetical situation of no AB in the ecosystem.
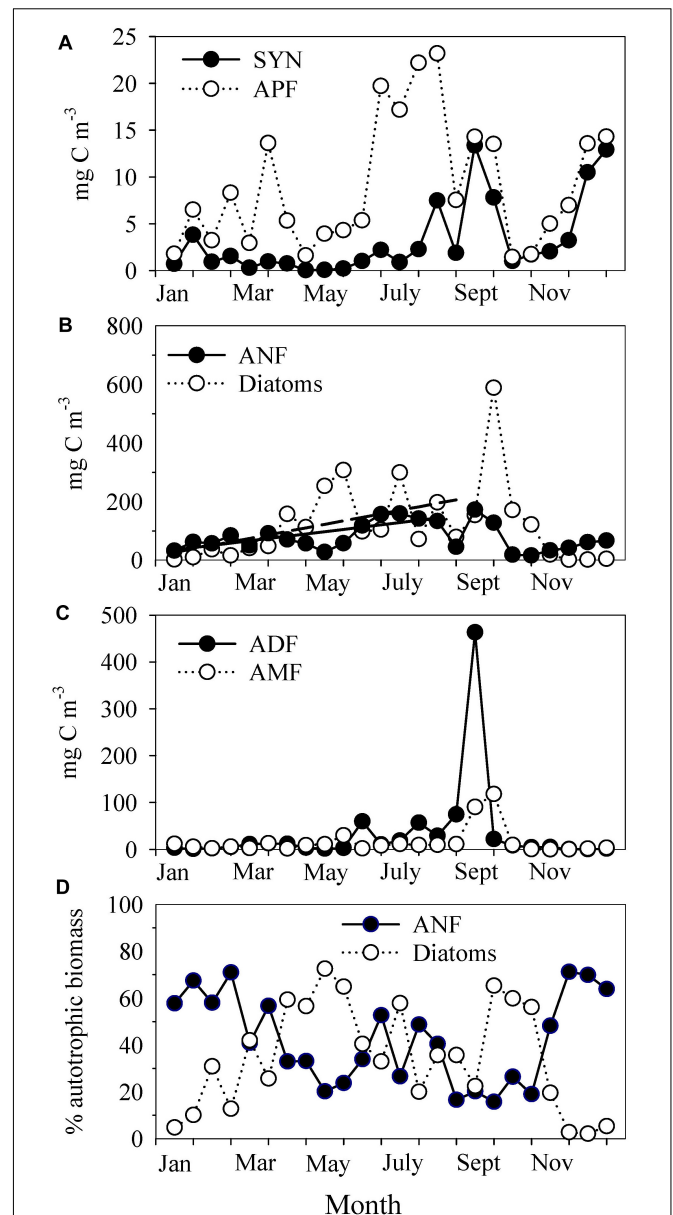
Autotrophic Components

Autotrophic picoflagellates (APF) and *Synechococcus* (SYN) (**Figure 5A**) were not important components of the microbial plankton community. Their biomasses always remained below 25 mg C m^{-3} and only accounted for $5 \pm 4\%$ (APF) and $2 \pm 3\%$ (SYN) of the AB. However, both groups showed an increasing trend at the end of the year (November–December) following a previous strong decrease in September-October. APF represented $14 \pm 1\%$ of the AB in December, and SYN represented $12 \pm 0.4\%$. The maximum values of APF were found in July and August, when upwelling relaxed (**Figure 2C**).

Diatoms and autotrophic nanoflagellates (ANF) were the plankton groups with the highest biomasses within the autotrophic community (**Figure 5B**). ANF, which were important all year (mean 81 ± 47 mg C m^{-3}), increased from ~30 mg C m^{-3} in January to ~155 mg C m^{-3} in the first half of August at a rate of 7 ± 2 mg C m^{-3} per half-month. Diatoms also experienced a similar seasonal trend to increase, but the rate was higher, 15 ± 5 mg C m^{-3} per half-month, an increasing trend that was disrupted by biomass peaks (**Figure 5B**). The mean ANF

FIGURE 4 | Time series of (A) total autotrophic biomass (AB) and total heterotrophic biomass (HB) of microbial plankton and (B) the relationship between the total AB and total HB of microbial plankton. In (A) the continuous line shows the seasonal increase of AB, $Y = (48 \pm 38) + (23 \pm 4)X$; $r^2 = 0.71$; $n = 16$; $p < 0.001$. Dashed line illustrates the seasonal increase of HB, $Y = (57 \pm 16) + (8 \pm 2)X$; $r^2 = 0.59$; $n = 16$; $p < 0.001$. In (B) the dashed line denotes the 1:1 relationship. The values were averaged every half-month ($n = 3–5$) to remove short-term variability.

FIGURE 5 | Time series of (A) the biomass of *Synechococcus* (SYN) and autotrophic picoflagellates (APF), (B) the biomass of autotrophic nanoflagellates (ANF) and diatoms, (C) the biomass of autotrophic dinoflagellates (ADF) and other autotrophic microflagellates (AMF), and (D) the contributions of ANFs and diatoms to the total AB. The continuous line in (B) depicts the seasonal increase in ANF: $Y = (27 \pm 17) + (7 \pm 2)X$; $r^2 = 0.56$; $n = 15$; $p = 0.001$. The dashed line shows the seasonal increase in diatoms: $Y = (-3 \pm 45) + (15 \pm 5)X$; $r^2 = 0.46$; $n = 15$; $p = 0.009$. The values were averaged every half-month ($n = 3–5$) to remove short-term variability.

biomass in winter (58 ± 18 mg C m^{-3}) was higher than the diatom biomass (10 ± 12 mg C m^{-3}). In contrast, the biomass of diatoms was considerably higher in May (diatoms 280 ± 38 mg C m^{-3}; ANF 47 ± 15 mg C m^{-3}) and during the second half of September (diatoms 589 mg C m^{-3}; ANF 172 mg C m^{-3}). Several *Chaetoceros* spp. dominated in May, whereas the maximum in September was almost exclusively composed of *Skeletonema* cf. *costatum* (435 mg C m^{-3}).

The biomasses of autotrophic dinoflagellates (ADF) and autotrophic microflagellates (AMF) were generally low (**Figure 5C**), with average contributions to the AB of 7 ± 11 and $5 \pm 5\%$, respectively. The mean biomass values in winter were 2.4 $\pm$ 1.8 mg C m^{-3} for ADF and 3.9 $\pm$ 3.9 mg C m^{-3} for AMF. Nevertheless, both groups peaked in September, up to 463 and 118 mg C m^{-3}, when their contributions to the AB increased to 50 and 13%, respectively. *Tripos muelleri*, formerly *Ceratium tripos* (228 mg C m^{-3}) and *T. fusus*, formerly *C. fusus* (72 mg C m^{-3}) were the two species with large contributions to the ADF maximum (65% of ADF biomass), whereas *Brachiomonas* sp.

(53 mg C m^{-3}), *Oltmannsiellopsis viridis* (43 mg C m^{-3}), and Cryptophyceae spp. (11 mg C m^{-3}) accounted for 91% of the AMF biomass in September.
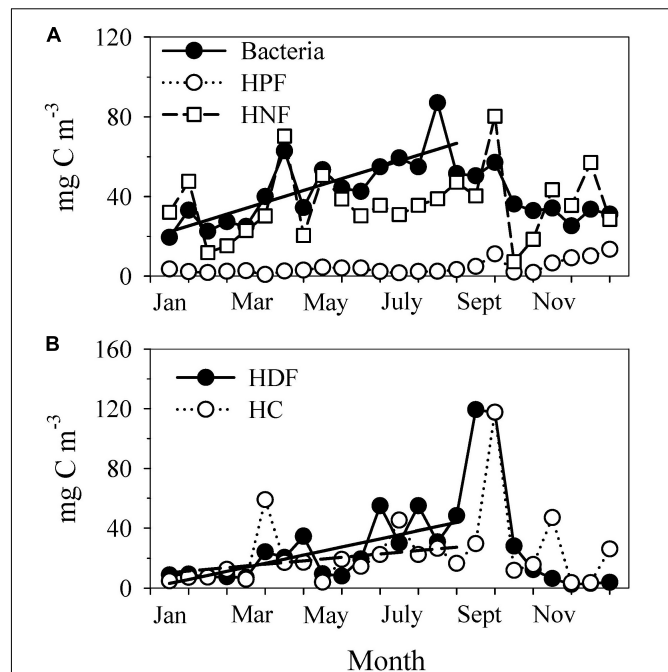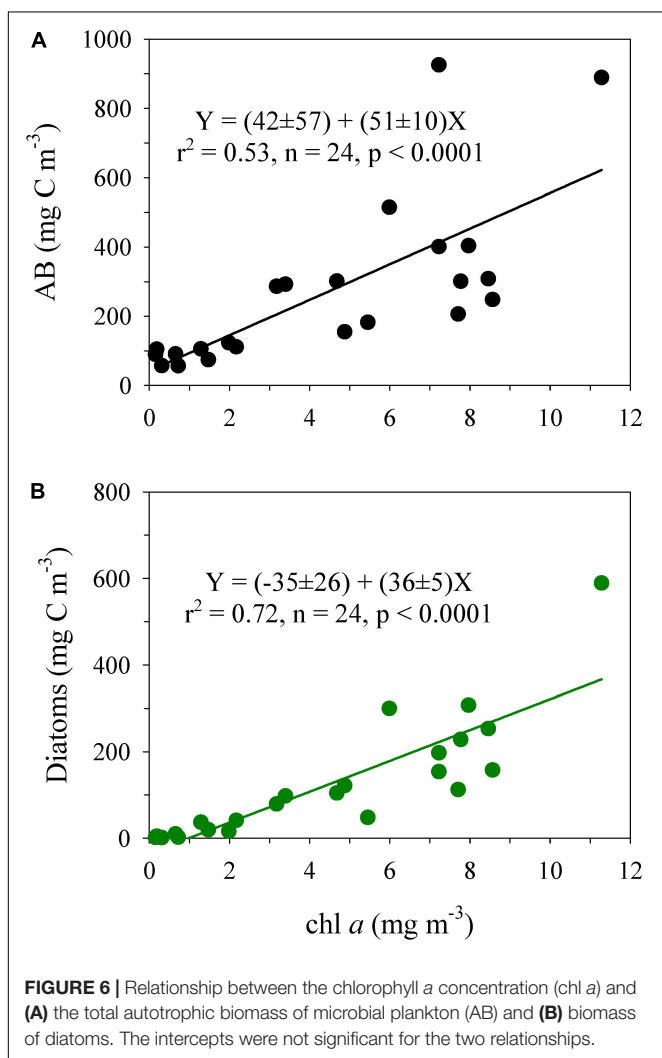
Autotrophic ciliates (data not shown) were a minor component of the microbial plankton community ($3 \pm 5\%$ of the total AB). Their presence in the community was occasional.

Diatoms and ANF accounted for 80 $\pm$ 18% of the AB, with opposite contributions throughout the year ($r = -0.83$, $p < 0.0001$) (**Figure 5D**). Whereas ANF dominated in winter (average contribution of 62 $\pm$ 7% to the AB), the dominance of diatoms was restricted to April-May and September–October, which coincided with the two chl a maxima (**Figure 2D**). Between June and the middle of August, when upwelling relaxed (**Figure 2C**), the contributions of diatoms (42 $\pm$ 11%) and ANF (42 $\pm$ 10%) to the AB were similar (**Figure 5D**).

Although the AB and chl a concentration were positively correlated (**Figure 6A**), as AB:chl a ratio (slope of the regression) = 51 $\pm$ 10 (w:w), the relationship noticeably improved, and the AB:chl a ratio decreased when only diatoms (36 $\pm$ 5) were considered in the autotrophic carbon biomass (**Figure 6B**). The correlation of ANF with the chl a concentration (**Supplementary Table S6**) was non-significant.

Heterotrophic Components

On an annual basis, bacteria and heterotrophic nanoflagellates (HNF) (**Figure 7A**) were the most important components

FIGURE 7 | Time series of **(A)** the biomass of heterotrophic bacteria (Bacteria), heterotrophic picoflagellates (HPF) and heterotrophic nanoflagellates (HNF) and **(B)** the biomass of heterotrophic dinoflagellates (HDF) and heterotrophic ciliates (HC). The continuous line in **(A)** describes the seasonal increase in heterotrophic bacteria: Y = (18 $\pm$ 6) + (3 $\pm$ 0.6)X; $r^2 = 0.62$; $n = 16$; $p = 0.0003$. In **(B)**, the continuous line denotes the seasonal increase in HDF: Y = (2 $\pm$ 6) + (2 $\pm$ 0.6)X; $r^2 = 0.49$; $n = 16$; $p = 0.002$. The dashed line shows the trend for HC that was not significant ($r^2 = 0.21$; $p = 0.071$). The values were averaged every half-month ($n = 3$–5) to remove short-term variability.

FIGURE 6 | Relationship between the chlorophyll a concentration (chl a) and **(A)** the total autotrophic biomass of microbial plankton (AB) and **(B)** biomass of diatoms. The intercepts were not significant for the two relationships.

of the heterotrophic community. Their average contributions were 36 $\pm$ 11 and 30 $\pm$ 12%, respectively. The bacterial biomass (average 42 $\pm$ 16 mg C m^{-3}) clearly increased from ~20 to ~60 mg C m^{-3} between January and the first half of August at a rate of 3 $\pm$ 0.6 mg C m^{-3} per half-month. From September onwards, the bacterial biomass dropped to the winter levels. The HNF biomass was also important throughout the year (36 $\pm$ 17 mg C m^{-3}), showing a significant correlation ($r = 0.48$, $p = 0.018$) with bacteria. However, this correlation was stronger in the first half of the year (January–June, $r = 0.75$, $p = 0.005$). HNF showed a tendency to increase at the end of the year following a strong decrease in the first fortnight of October. This increase coincided with that observed for autotrophic picoplankton (SYN and APF, **Figure 5A**). Heterotrophic picoflagellates (HPF), which did not reach important biomass values (4 $\pm$ 3 mg C m^{-3}, **Figure 7A**), also showed significantly higher biomasses ($p < 0.001$, t-test for two samples) at the end of the period of observations (November–December, 10 $\pm$ 3 mg C m^{-3}) than before.

Heterotrophic dinoflagellates (HDF) and heterotrophic ciliates (HC) (**Figure 7B**) followed a similar trend over time (HDF vs. HC, $r = 0.62$, $p = 0.001$), characterized by low biomass values during winter (6 $\pm$ 3 and 9 $\pm$ 8 mg C m^{-3}, respectively)
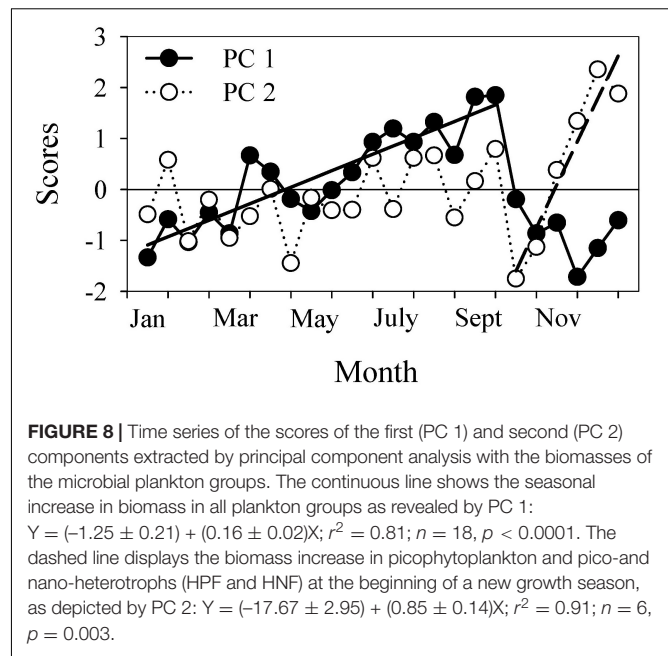
and the highest values during summer, especially at the end of the upwelling season in September (119 and 117 mg C m^{-3}, respectively). This seasonal trend was, however, more evident for HDF than for HC. The September maximum of HDF was caused by a mixed assemblage of *Protoperidinium* spp., *Gyrodinium fusiforme* and *Gymnodinium* spp. while *Codonellopsis* sp. accounted for 42% of the HC biomass. The contribution of HDF to the HB was the third in importance (19 ± 13%), following bacteria and HNF. The average contribution of HC was 16 ± 9%.

Principal Component Analysis

According to the results of PCA, 61% of the variability in the microbial plankton biomass in the surface layer of the Ría de Vigo could be explained by two components (**Table 1**). The first component (PC 1) showed the strongest positive loads with the biomasses of all microplankton components, bacteria, ANF and APF and was responsible for 41% of the total variability. The second component (PC 2), which showed the highest positive loads with SYN, APF, HPF and HNF, accounted for 20% of the additional variability. The PC 1 scores increased linearly from January to September, while the PC 2 scores, which varied irregularly around the zero line during this period, increased linearly between October and December when PC 1 dropped to negative scores (**Figure 8**). Although the PC 1 scores remained negative in December, they showed a tendency to increase following the increase hitherto depicted by PC 2 (**Figure 8**).

DISCUSSION

Although short-term variability is characteristic of coastal upwelling systems, and spatial variability can be relevant in bays, seasonality revealed as a very distinctive feature in this temperate ecosystem. Upwelling-favorable winds (positive values of −Qx) from April to September (**Figure 2C**), when solar radiation was high (**Figure 2A**) and runoff was low

FIGURE 8 | Time series of the scores of the first (PC 1) and second (PC 2) components extracted by principal component analysis with the biomasses of the microbial plankton groups. The continuous line shows the seasonal increase in biomass in all plankton groups as revealed by PC 1: $Y = (-1.25 \pm 0.21) + (0.16 \pm 0.02)X$; $r^2 = 0.81$; $n = 18$, $p < 0.0001$. The dashed line displays the biomass increase in picophytoplankton and pico- and nano-heterotrophs (HPF and HNF) at the beginning of a new growth season, as depicted by PC 2: $Y = (-17.67 \pm 2.95) + (0.85 \pm 0.14)X$; $r^2 = 0.91$; $n = 6$, $p = 0.003$.

TABLE 1 | Loads of the biomasses of the different microbial plankton groups with the first two principal components (PC 1, PC 2).

Variable	PC 1	PC 2
SYN	0.23	0.66
APF	0.63	0.66
ANF	0.78	0.26
HPF	−0.17	0.66
HNF	0.32	0.61
Bacteria	0.83	0.14
Diatoms	0.73	−0.49
ADF	0.79	−0.29
AMF	0.69	−0.13
HDF	0.90	−0.26
HC	0.76	−0.01

PC 1 and PC 2 explained 41 and 20% of the total variance, respectively. SYN, Synechococcus; APF, autotrophic picoflagellates; ANF, autotrophic nanoflagellates; HPF, heterotrophic picoflagellates; HNF, heterotrophic nanoflagellates; ADF, autotrophic dinoflagellates; AMF, autotrophic microflagellates; HDF, heterotrophic dinoflagellates; HC, heterotrophic ciliates.

(**Figure 2B**), brought nutrients to the surface waters of the Ría, where they were rapidly consumed by phytoplankton (**Figure 2D**). This variability has been previously reported for the Rías Baixas (Nogueira et al., 1997; Crespo et al., 2006), which typically displays two contrasting transitional periods in spring and autumn. The spring transition (April–May) occurred when the nutrients of continental origin were still abundant (**Figure 2D**); solar radiation began to increase (**Figure 2A**), and upwelling supplied additional nutrients (**Figure 2C**). All of these factors induced the spring bloom, which spanned approximately 2 months (**Figure 2D**). In contrast, the autumn transition (September–October) occurred when upwelling-favorable winds relaxed and westerly winds (negative values of Qy) were more important (**Figure 2C**). This phenomenon caused a reversal of circulation that resulted in the rapid accumulation of plankton in the interior of the Ría (**Figures 2D**, **4A**) before leading to winter conditions that were characterized by high nutrient concentrations and low plankton levels. The sudden accumulation of plankton during the autumn transition was due to plankton advection toward the interior of the Ría, plankton that was previously transported toward the shelf by prevailing estuarine-like upwelling circulation (Figueiras et al., 1994; Tilstone et al., 1994; Fermín et al., 1996). This rapid accumulation contrasted with the more progressive plankton increase observed previously, in spring and summer, which was mainly attributable to local growth (**Figure 4A**).

The reorganization of the microbial plankton community that followed the sudden decay in biomass caused by the autumn transition (**Figure 4A**) began with the increase of the small phytoplankton forms (SYN and APF; **Figure 5A**) plus pico- (HPF) and nano-heterotroph (HNF) (**Figure 7A**) (PC 2 in **Table 1** and **Figure 8**). This type of response by microbial plankton communities has been reported

elsewhere (Landry, 2002; Barber and Hiscock, 2006; Espinoza-González et al., 2012; Paulsen et al., 2017) and corresponds to the onset of the new growing season (around January, **Figure 8**) that precedes the spring bloom. It has been explained by the intrinsically high growth rate of picophytoplankton (Agawin et al., 2000; Barber and Hiscock, 2006). Large phytoplankton will succeed later on (PC 1 in **Figure 8**), when picophytoplankton begin to be controlled by their grazers (HNF and HPF), which are always present in the microbial community (Teixeira et al., 2011).

Although mixotrophic nutrition can occur within pigmented nanoflagellates (Unrein et al., 2007; Zubkov and Tarran, 2008; Crespo et al., 2011) and pigmented dinoflagellates (Stoecker, 1999; Skovgaard et al., 2000), the dominance of autotrophs during the whole upwelling season (**Figure 4A**; April to October) and the codominance of autotrophs and heterotrophs in winter are consistent with the metabolic rates of the microbial community determined in this coastal ecosystem (Moncoiffé et al., 2000; Cermeño et al., 2006; Arbones et al., 2008). These studies reported autotrophy during the upwelling season and a metabolic balance (production = respiration) during winter. The prevalence of autotrophic metabolism in this semienclosed bay during the upwelling season contrasts with the situation found in the adjacent shelf and oceanic waters (Teira et al., 2001; Espinoza-González et al., 2012), where autotrophy was recorded only during short-term upwelling events that usually occur within the upwelling season. As the dominance of autotrophic metabolism in microbial communities is related to the nutrient supply (Buck et al., 1996; Gasol et al., 1997; Duarte et al., 2000), it can be inferred that upwelling is continuously supplying nutrients to the Ría. In fact, upwelling is considerably enhanced in the Ría (Figueiras et al., 2002; Crespo et al., 2007) because its bathymetric configuration, which is shallow in the inner part (**Figure 1**), favors the intrusion of upwelled subsurface water onto the shelf. As a result, a weak upwelling with no or slight effects on the shelf is strong enough to bring nutrients into the Ría and fuel phytoplankton growth (Figueiras et al., 2002), as suggested by the low phytoplankton carbon to chl *a* ratios recorded (**Figure 6**) (Geider et al., 1998; Taylor et al., 2015). The persistence of upwelling inside the Ría was also

inferred from the constant presence of diatoms in its waters, as diatoms regularly thrive following upwelling events (Varela et al., 1991; Anabalón et al., 2007; Espinoza-González et al., 2012; Taylor et al., 2015). Despite the dominance of autotrophs, the covariance of autotrophs and heterotrophs (**Figure 4B**) indicates the tight coupling between both components of the microbial community; multiple trophic relationships were established (Teixeira et al., 2011), with heterotrophs quickly responding to the proliferation of autotrophs.

The continuous increase observed in the biomass of virtually all components of the microbial community during the upwelling season (**Table 1** and **Figure 8**) and specifically the increase in AB (**Figure 4A**) indicate the occurrence of an increase in nutrients injected into the Ría (**Figure 3A**) despite the reduction in upwelling intensity from May onwards (**Figure 2C**). Certainly, it can be argued that weak upwelling slowed circulation in the estuary, therefore favoring the accumulation (through diminishing oceanwards transport) of phytoplankton inside the Ría. However, weak circulation should also cause nutrient depletion by favoring phytoplankton consumption and thus preventing the continuous increase in AB. In addition, heterotrophic consumption within the microbial community will cause a reduction in AB and an increase in HB, leading to a shift in the HB:AB ratio over the upwelling season, which was not observed (**Figure 4B**). Hence, a constant increase in nutrient supply must be the main process responsible for the observed increase in plankton biomass. Since both runoff and upwelling decreased throughout the season, the increase in the nutrient supply was possible only through nutrient regeneration at the sediment-water interface. The benthic regeneration of sinking material is important inside the Ría (Alonso-Pérez and Castro, 2014), where benthic remineralized nitrogen and phosphorous may represent up to 40–60% of the nutrients supplied by the sum of upwelled and continental waters throughout the year. At the same time, whereas transported by estuarine-like circulation, a significant portion of the material sinks to the bottom in the outermost part of the Ría and in the adjacent shelf, where intense regeneration processes occur. Successive upwelling events reintroduce these regenerated nutrients into the Ría, causing the nutrient enrichment of upwelled waters

TABLE 2 | Linear regressions between the nutrient concentrations [nitrate (NO_3^-); ammonium (NH_4^+); total dissolved inorganic nitrogen (DIN); phosphate (HPO_4^{2-}); silicate ($Si(OH)_4$)] in the bottom layer and the time (half-month) from March to September in the middle of the Ría de Vigo in 1991 and in 1987.

Year	Nutrient	Intercept	Slope	Regression coefficient
1991	NO_3^-	4.98 ± 1.14 ($p = 0.001$)	0.24 ± 0.13 ($p = 0.099$)	$r^2 = 0.21$
	NH_4^+	1.20 ± 0.78 ($p = 0.146$)	0.21 ± 0.09 ($p = 0.039$)	$r^2 = 0.31$
	DIN	6.55 ± 0.59 ($p < 0.0001$)	0.48 ± 0.07 ($p < 0.0001$)	$r^2 = 0.80$
	HPO_4^{2-}	0.33 ± 0.05 ($p < 0.0001$)	0.05 ± 0.01 ($p < 0.0001$)	$r^2 = 0.88$
	$Si(OH)_4$	2.46 ± 1.3 ($p = 0.082$)	0.55 ± 0.15 ($p = 0.004$)	$r^2 = 0.52$
1987	NO_3^-	3.14 ± 1.05 ($p = 0.011$)	0.39 ± 0.12 ($p = 0.008$)	$r^2 = 0.46$
	NH_4^+	0.93 ± 0.53 ($p = 0.105$)	0.18 ± 0.06 ($p = 0.015$)	$r^2 = 0.40$
	DIN	4.39 ± 1.15 ($p = 0.002$)	0.60 ± 0.14 ($p = 0.001$)	$r^2 = 0.62$
	HPO_4^{2-}	0.22 ± 0.07 ($p = 0.01$)	0.06 ± 0.01 ($p < 0.0001$)	$r^2 = 0.81$
	$Si(OH)_4$	3.16 ± 0.45 ($p < 0.0001$)	0.55 ± 0.05 ($p < 0.0001$)	$r^2 = 0.90$

n = 14.

(**Figure 3A**) (Álvarez-Salgado et al., 1997; Crespo et al., 2006). Previous studies have shown that up to 50% of the nitrate and 80% of the silicate supplied to the Ría by upwelled water at the end of the upwelling season originated from this type of regeneration (Álvarez-Salgado et al., 1997). The nutrients in the bottom layer determined during this sampling (**Figure 3A**) and during a previous sampling performed at the same location in the Ría clearly showed a gradual increase in nutrient levels over time (**Table 2**). Using these relationships and considering that this increase in nutrient concentrations was only due to regeneration processes in the system, it can be deduced that regenerated nutrients at the end of the upwelling season (slope x 14 fortnights) could represent between 40% for nitrate and 76% for silicate of the total nutrients supplied to the Ría by upwelling circulation (slope x 14 + intercept) during our sampling year. These values were similar to those obtained for the preceding sampling in 1987, when regenerated nutrients at the end of the upwelling season varied between 64% for nitrate and 79% for phosphate of the total nutrients supplied.

The occurrence of nutrient regeneration can also be inferred by looking at the concentrations of ammonium and nitrate in the bottom layer (**Figure 3A**). Both nutrients show increases in their concentrations between March and September, but ammonium with lower concentrations. This can occur because ammonium is the first inorganic product in the regeneration of nitrogen, which will end with the accumulation of its most oxidized form: nitrate. The same trend for both nutrients but with a lower ammonium concentration, as well as the coincidence of ammonium peaks and nitrate valleys in June and September points to the existence of important nitrogen regeneration processes in the bottom layer of the Ría. Therefore, it can be concluded that the Rías and the adjacent shelf act as a nutrient trap that efficiently recycles nutrients to allow the continuous increase in microbial plankton biomass and, more specifically, the increase in phytoplankton biomass during the upwelling season. Therefore, recycling and nutrient trapping are two processes that significantly contribute to explaining the high productivity of the Rías (Moncoiffé et al., 2000; Cermeño et al., 2006; Arbones et al., 2008), allowing these semienclosed bays to be the coastal region with the highest mussel production in Europe (Figueiras et al., 2002). Environmental or human-induced changes that modify these oceanographic conditions can result in important reductions in mussel production that would significantly affect the economy of the region. Thus, this study performed three decades ago becomes an important snapshot of the system that can be immediately compared with more recent or future studies in order to find changes that maybe already occurring in the system.

DATA AVAILABILITY STATEMENT

All datasets generated for this study are included in the article/**Supplementary Material**.

AUTHOR CONTRIBUTIONS

FF wrote the manuscript and designed the research in collaboration with IT. All authors contributed to data interpretation, discussion of the results, and assisted in the writing process revising the manuscript. All authors contributed to the article and approved the submitted version.

FUNDING

ACKNOWLEDGMENTS

SUPPLEMENTARY MATERIAL

The Supplementary Material for this article can be found online at: https://www.frontiersin.org/articles/10.3389/fmars.2020.578042/full#supplementary-material

REFERENCES

Agawin, N. S. R., Duarte, C. M., and Agustí, S. (2000). Nutrient and temperature control of the contribution of picoplankton to phytoplankton biomass and production. *Limnol. Oceanogr.* 45, 591–600. doi: 10.4319/lo.2000.45.3.0591

Alonso-Pérez, F., and Castro, C. G. (2014). Benthic oxygen and nutrient fluxes in a coastal upwelling system (Ria de Vigo, NW Iberian Peninsula): seasonal trends and regulating factors. *Mar. Ecol. Progr. Ser.* 511, 17–32. doi: 10.3354/meps10915

Álvarez-Salgado, X. A., Borges, A. V., Figueiras, F. G., and Chou, L. (2010). "Iberian margin: the Rías," in *Carbon and Nutrient Fluxes in Continental Margins:*

A Global Synthesis, eds K. K. Liu, L. Atkinson, R. Quiñones, and L. Talaue Mac-Manus (Berlin Heidelberg: Springer Verlag), 103–120.

Álvarez-Salgado, X. A., Castro, C. G., Pérez, F. F., and Fraga, F. (1997). Nutrient mineralization patterns in shelf waters of the Western Iberian upwelling. *Cont. Shelf Res.* 17, 1247–1270. doi: 10.1016/S0278-4343(97)00014-9

Anabalón, V., Morales, C. E., Escribano, R., and Varas, M. A. (2007). The contribution of nano- and micro-planktonic assemblages in the surface layer (0-30m) under different hydrographic conditions in the upwelling area off Concepción, central Chile. *Prog. Oceanogr.* 75, 396–414. doi: 10.1016/j.pocean.2007.08.023

Arbones, B., Castro, C. G., Alonso-Pérez, F., and Figueiras, F. G. (2008). Phytoplankton size structure and water column metabolic balance in a coastal

upwelling system: the Ría de Vigo. NW Iberia. *Aquat. Microb. Ecol.* 50, 169–179. doi: 10.3354/ame01160

Bakun, A. (1973). *Coastal Upwelling Indices, West Coast of North America 1946-1971*. NOAA Technical Report, NMFS SSRF-671. Washington DC: US Department of Commerce.

Barber, R. T., and Hiscock, M. R. (2006). A rising tide lifts all phytoplankton: growth response of other phytoplankton taxa in diatom-dominated blooms. *Global Biogeochem. Cycles* 20, GB4S03. doi: 10.1029/2006GB002726

Barton, E. D., Largier, J. L., Torres, R., Sheridan, M., Trasviña, A., Souza, A., et al. (2015). Coastal upwelling and downwelling forcing of circulation in a semi-enclosed bay: ría de Vigo. *Prog. Oceanogr.* 134, 173–189. doi: 10.1016/j.pocean.2015.01.014

Barton, E. D., Torres, R., Figueiras, F. G., Gilcoto, M., and Largier, J. (2016). Surface water subduction during a downwelling event in a semienclosed bay. *J. Geophys. Res. Oceans* 121, 7088–7107. doi: 10.1002/2016JC011950

Bauer, J. E., Cai, W. J., Raymond, P. A., Bianchi, T. S., Hopkinson, C. S., and Regnier, P. A. G. (2013). The changing carbon cycle of the coastal ocean. *Nature* 504, 61–70. doi: 10.1038/nature12857

Billen, G. (1978). A budget of nitrogen recycled in North Sea sediments off the Belgian coast. *Estuar. Coast. Mar. Sci.* 7, 127–146. doi: 10.1016/0302-3524(78)90070-1

Blanton, J. O., Atkinson, L. P., Fernández de Castillejo, F., and Lavín, A. (1984). Coastal upwelling off the rías bajas, Galicia, Northwest Spain, I: hydrography studies. *Rapp P-v. réun. Cons. Int. explor. Mer.* 183, 79–90.

Blanton, J. O., Tenore, K. R., Castillejo, F., Atkinson, L. P., Schwing, F. B., and Lavin, A. (1987). The relationship of upwelling to mussel production in the rias on the western coast of Spain. *J. Mar. Res.* 45, 497–511. doi: 10.1357/002224087788401115

Boynton, W. R., Ceballos, M. A. C., Bailey, E. M., Hodgkins, C. L. S., Humphrey, J. L., and Testa, J. M. (2018). Oxygen and nutrient exchanges at the sediment-water interface: a global synthesis and critique of estuarine and coastal data. *Estuar. Coast.* 41, 301–333. doi: 10.1007/s12237-017-0275-5

Bratbak, G., and Dundas, I. (1984). Bacterial dry matter content and biomass estimation. *Appl. Environ. Microbiol.* 48, 755–775.

Buck, K. R., Chavez, F. P., and Campbell, L. (1996). Basin-wide distributions of living carbon components and the inverted trophic pyramid of the central gyre of the North Atlantic Ocean, summer 1993. *Aquat. Microb. Ecol.* 10, 283–298. doi: 10.3354/ame010283

Cermeño, P., Marañón, E., Pérez, V., Serret, P., Fernández, E., and Castro, C. G. (2006). Phytoplankton size structure and primary production in a highly dynamic coastal ecosystem (Ría de Vigo, NW Spain): seasonal and short-time scale variability. *Estuar. Coast. Shelf. Sci.* 67, 251–256. doi: 10.1016/j.ecss.2005.11.027

Cloern, J. E., Abreu, P. C., Carstensen, J., Chauvaud, L., Elmgren, R., Grall, J., et al. (2016). Human activities and climate variability drive fast-paced change across the world's estuarine–coastal ecosystems. *Glob. Change Biol.* 22, 513–529. doi: 10.1111/gcb.13059

Cohen, J. E., Small, C., Mellinger, A., Gallup, J., Sachs, J., Vitouseck, P. M., et al. (1997). Estimates of coastal populations. *Science* 278, 1209–1213. doi: 10.1126/science.278.5341.1209c

Crespo, B. G., Espinoza-González, O., Teixeira, I. G., Castro, C. G., and Figueiras, F. G. (2011). Possible mixotrophy of pigmented nanoflagellates: microbial plankton biomass, primary production and phytoplankton growth at the NW Iberian upwelling in spring. *Estuar. Coast. Shelf Sci.* 94, 172–181. doi: 10.1016/j.ecss.2011.06.008

Crespo, B. G., Figueiras, F. G., and Groom, S. (2007). Role of across-shelf currents in the dynamics of harmful dinoflagellate blooms in the northwestern Iberian upwelling. *Limnol. Oceanogr.* 52, 2668–2678. doi: 10.4319/lo.2007.52.6.2668

Crespo, B. G., Figueiras, F. G., Porras, P., and Teixeira, I. G. (2006). Downwelling and dominance of autochthonous dinoflagellates in the NW Iberian margin: the example of the Ría de Vigo. *Harmful Algae* 5, 770–781. doi: 10.1016/j.hal.2006.03.006

Dietrich, G., Kalle, K., Kraus, W., and Siedler, G. (1980). *General Oceanography. An introduction*, 2nd Edn. New York, NY: John Wiley and Sons.

Duarte, C. M., Agustí, S., Gasol, J. M., Vaqué, D., and Vázquez-Domínguez, E. (2000). Effect of nutrient supply on the biomass structure of planktonic communities: an experimental test on a Mediterranean coastal community. *Mar. Ecol. Progr. Ser.* 206, 87–95. doi: 10.3354/meps206087

Edler, L. (1979). Recommendations for marine biological studies in the Baltic Sea. Phytoplankton and Chlorophyll. *Baltic Mar. Biol.* 5, 1–38.

Espinoza-González, O., Figueiras, F. G., Crespo, B. G., Teixeira, I. G., and Castro, C. G. (2012). Autotrophic and heterotrophic microbial plankton biomass in the NW Iberian upwelling: seasonal assessment of metabolic balance. *Aquat. Microb. Ecol.* 67, 77–89. doi: 10.3354/ame01584

Fermín, E. G., Figueiras, F. G., Arbones, B., and Villarino, M. L. (1996). Short-time scale development of a Gymnodinium catenatum population in the Ría de Vigo (NW Spain). *J. Phycol.* 32, 212–221. doi: 10.1111/j.0022-3646.1996.00212.x

Fernández, E., Álvarez-Salgado, X. A., Beiras, R., Ovejero, A., and Méndez, G. (2016). Coexistence of urban uses and shellfish production in an upwelling-driven, highly productive marine environment: the case of the Ría de Vigo (Galicia. Spain). *Reg. Stud. Mar. Sci.* 8, 362–370. doi: 10.1016/j.rsma.2016.04.002

Figueiras, F. G., Espinoza-González, O., Arbones, B., Garrido, J. L., Teixeira, I. G., and Castro, C. G. (2014). Estimating phytoplankton size-fractionated primary production in the northwestern Iberian upwelling: is mixotrophy relevant in pigmented nanoplankton? *Prog. Oceanogr.* 128, 88–97. doi: 10.1016/j.pocean.2014.08.011

Figueiras, F. G., Jones, K. J., Mosquera, A. M., Álvarez-Salgado, X. A., Edwards, A., and MacDougall, N. (1994). Red tide assemblage formation in an estuarine upwelling ecosystem: ría de Vigo. *J. Plankton Res.* 16, 857–878. doi: 10.1093/plankt/1607.857

Figueiras, F. G., Labarta, U., and Fernández Reiriz, M. J. (2002). Coastal upwelling, primary production and mussel growth in the Rías Baixas of Galicia. *Hydrobiologia* 484, 121–131. doi: 10.1023/A:1021309222459

Fraga, S., Anderson, D. M., Bravo, I., Reguera, B., Steindinger, K. A., and Yentsch, C. M. (1988). Influence of upwelling relaxation on dinoflagellates and shellfish toxicity in Ría de Vigo. *Spain. Estuar. Coast. Shelf Sci.* 27, 349–361. doi: 10.1016/0272-7714(88)90093-5

Froján, M., Arbones, B., Zúñiga, D., Castro, C. G., and Figueiras, F. G. (2014). Microbial plankton community in the Ría de Vigo (NW Iberian upwelling system): impact of the culture of *Mytilus galloprovincialis*. *Mar. Ecol. Prog. Ser.* 498, 43–54. doi: 10.3354/meps10612

Gasol, J. M., del Giorgio, P. A., and Duarte, C. M. (1997). Biomass distribution in marine planktonic communities. *Limnol. Oceanogr.* 42, 1353–1363. doi: 10.4319/lo.1997.42.6.1353

Geider, R. J., MacIntyre, H. L., and Kana, T. M. (1998). A dynamic regulatory model of phytoplankton acclimation to light, nutrients and temperature. *Limnol. Oceanogr.* 43, 679–694. doi: 10.4319/lo.1998.43.4.0679

Grasshoff, K., and Johannsen, H. (1972). A new sensitive and direct method for the automatic determination of ammonia in seawater. *ICES J. Mar. Sci.* 34, 516–521. doi: 10.1093/icesjms/34.3.516

Hansen, H. P., and Grasshoff, K. (1983). "Automated chemical analysis," in *Methods in Seawater Analysis*, eds K. Grasshoff, M. Ehrardt, and K. Kermling (Weinhein: Verlag Chemie), 347–379.

Hinrichsen, D. (1994). Coasts under pressure. *People Planet* 3, 6–9.

Holligan, P., and de Boois, H. (1993). *Land Ocean Interactions in the Coastal Zone (LOICZ) Science Plan*, IGBP Report No. 2. Stockholm: IGBP.

Huntington, T., Nimmo, F., and Macfadyen, G. (2015). Fish landings at the world's commercial fishing ports. *J. Ocean Coastal Econ.* 2:4. doi: 10.15351/2373-8456.1031

Jickells, T. D. (1998). Nutrient biogeochemistry of the coastal zone. *Science* 281, 217–222. doi: 10.1126/science.281.5374.217

Landry, M. R. (2002). Integrating classical and microbial food web concepts: evolving views from the open-ocean tropical Pacific. *Hydrobiologia* 480, 29–39. doi: 10.1023/A:1021272731737

Lee, S., and Fuhrman, J. A. (1987). Relationships between biovolume and biomass of naturally derived marine bacterioplankton. *Appl. Environ. Microbiol.* 53, 1298–1303.

Lessard, E. J., and Swift, E. (1986). Dinoflagellates from the North Atlantic classified as phototrophic or heterotrophic by epifluorescence microscopy. *J. Plankton Res.* 8, 1209–1215. doi: 10.1093/plankt/8.6.1209

Lubchenco, J., and Petes, L. E. (2010). The Interconnected Biosphere: science at the Ocean's Tipping Points. *Oceanography* 23, 115–129. doi: 10.5670/oceanog.2010.55

Millennium Ecosystem Assessment (2005). *Ecosystems and Human Well-Being: Synthesis*. Washington, DC: Island Press.

Moncoiffé, G., Álvarez-Salgado, X. A., Figueiras, F. G., and Savidge, G. (2000). Seasonal and short-time scale dynamics of microplankton community production and respiration in an inshore upwelling system. *Mar. Ecol. Prog. Ser.* 196, 111–126. doi: 10.3354/meps196111

Mouriño, C., and Fraga, F. (1985). Determinación de nitratos en agua de mar. *Invest. Pesq.* 49, 81–96.

Nogueira, E., and Figueiras, F. G. (2005). The microplankton succession in the Ría de Vigo revisited: species assemblages and the role of the weather-induced, hydrodynamic variability. *J. Mar. Syst.* 54, 139–155. doi: 10.1016/j.jmarsys.2004.07.009

Nogueira, E., Ibanez, F., and Figueiras, F. G. (2000). Effect of meteorological and hydrographic disturbances on the microplankton community structure in the Ría de Vigo (NW Spain). *Mar. Ecol. Prog. Ser.* 203, 23–45. doi: 10.1006/ecss.1996.0119

Nogueira, E., Pérez, F. F., and Ríos, A. F. (1997). Seasonal patterns and long-term trends in an estuarine upwelling ecosystem (Ría de Vigo. NW Spain). *Estuar. Coast. Shelf Sci.* 44, 285–300. doi: 10.1006/ecss.1996.0119

Paulsen, M. L., Riisgaard, K., St. John, M., Thingstad, T. F., and Nielsen, T. G. (2017). Heterotrophic nanoflagellate grazing facilitates subarctic Atlantic spring bloom development. *Aquat. Microb. Ecol.* 78, 161–176. doi: 10.3354/ame01807

Piedracoba, S., Álvarez-Salgado, X. A., Rosón, G., and Herrera, J. L. (2005). Short-timescale thermohaline variability and residual circulation in the central segment of the coastal upwelling system of the Ría de Vigo (northwest Spain) during four contrasting periods. *J. Geophys. Res. Oceans* 110, C03018. doi: 10.1029/2004JC002556

Porter, K. G., and Feig, Y. S. (1980). The use of DAPI for identifying and counting aquatic microflora. *Limnol. Oceanogr.* 25, 943–948. doi: 10.4319/lo.1980.25.5.0943

Putt, M., and Stoecker, D. K. (1989). An experimental determined carbon:volume ratio for marine "oligotrichous" ciliates from estuarine and coastal waters. *Limnol. Oceanogr.* 34, 1097–1103. doi: 10.4319/lo.1989.34.6.1097

Ríos, A. F., Nombela, M., Pérez, F. F., Rosón, G., and Fraga, F. (1992). Calculation of runoff to an estuary. Ría de Vigo. *Sci. Mar.* 56, 29–33.

Rodríguez, F., Pazos, Y., Maneiro, J., and Zapata, M. (2003). Temporal variation in phytoplankton assemblages and pigment composition at a fixed station of the Ría of Pontevedra. *Estuar. Coast. Shelf Sci.* 58, 499–515. doi: 10.1016/S0272-7714(03)00130-6

Sale, P. F., Agardy, T., Ainsworth, C. H., Feist, B. E., Bell, J. D., Christie, P., et al. (2014). Transforming management of tropical coastal seas to cope with challenges of the 21st century. *Mar. Poll. Bull.* 85, 8–23. doi: 10.1016/j.marpolbul.2014.06.005

Sanders, R. W., Caron, D. A., Davidson, J. M., Dennett, M. R., and Moran, D. M. (2001). Nutrient acquisition and population growth of a mixotrophic alga in axenic and bacterized Cultures. *Microb. Ecol.* 42, 513–523. doi: 10.1007/s00248-001-1024-6

Skovgaard, A., Hansen, P. J., and Stoecker, D. A. (2000). Physiology of the mixotrophic dinoflagellate fragilidium subglobosum. I. Effects of phagotrophy and irradiance on photosynthesis and carbon content. *Mar. Ecol. Prog. Ser.* 201, 129–136. doi: 10.3354/meps201129

Stoecker, D. K. (1999). Mixotrophy among dinofagellates. *J. Eukaryot. Microbiol.* 46, 397–401. doi: 10.1111/j.1550-7408.1999.tb04619.x

Strathmann, R. (1967). Estimating the organic carbon content of phytoplankton from cell volume or plasma volume. *Limnol. Oceanogr.* 12, 411–418. doi: 10.4319/lo.1967.12.3.0411

Taylor, A. G., Landry, M. R., Selph, K. E., and Wokuluk, J. J. (2015). Temporal and spatial patterns of microbial community biomass and composition in the southern california current ecosystem. *Deep Sea Res. II* 112, 117–128. doi: 10.1016/j.dsr2.2014.02.006

Teira, E., Serret, P., and Fernández, E. (2001). Phytoplankton size-structure, particulate and dissolved organic carbon production and oxygen fluxes through microbial communities in the NW Iberian coastal transition zone. *Mar. Ecol. Prog. Ser.* 219, 65–83. doi: 10.3354/meps219065

Teixeira, I. G., Figueiras, F. G., Crespo, B. G., and Piedracoba, S. (2011). Microzooplankton feeding impact in a coastal upwelling system on the NW Iberian margin: the Ría de Vigo. *Estuar. Coast. Shelf Sci.* 91, 110–120. doi: 10.1016/j.ecss.2010.10.012

Tilstone, G. H., Figueiras, F. G., Fermín, E. G., and Arbones, B. (1999). Significance of nanophytoplankton photosynthesis and primary production in a coastal upwelling system (Ria de Vigo. NW Spain). *Mar. Ecol. Prog. Ser.* 183, 13–27. doi: 10.3354/meps183013

Tilstone, G. H., Figueiras, F. G., and Fraga, F. (1994). Upwelling-downwelling sequences in the generation of red tides in a coastal upwelling system. *Mar. Ecol. Prog. Ser.* 112, 241–253.

Unrein, F., Massana, R., Alonso-Sáez, L., and Gasol, J. M. (2007). Significant year-round effect of small mixotrophic flagellates on bacterioplankton in an oligotrophic coastal system. *Limnol. Oceanogr.* 52, 456–469. doi: 10.4319/lo.2007.52.1.0456

Varela, M., Díaz del Río, G., Álvarez-Ossorio, M. T., and Costas, E. (1991). Factors controlling phytoplankton size class distribution in the upwelling area of the Galician continental shelf (NW Spain). *Sci. Mar.* 55, 505–518.

Verity, P. G., Robertson, C. Y., Tronzo, C. R., Andrews, M. G., Nelson, J. R., and Sieracki, M. E. (1992). Relationships between cell volume and the carbon and nitrogen content of marine photosynthetic nanoplankton. *Limnol. Oceanogr.* 37, 1434–1446. doi: 10.4319/lo.1992.37.7.1434

Wollast, R. (1998). "Evaluation and comparison of the global carbon cycle in the coastal zone and in the open ocean," in *The Sea*, eds K. H. Brink and A. R. Robinson (New York: John Wiley & Sons), 213–252.

Wooster, W. S., Bakun, A., and McLain, D. R. (1976). The seasonal upwelling cycle along the eastern boundary of the North Atlantic. *J. Mar. Res.* 34, 131–141.

Yentsch, C. S., and Menzel, D. W. (1963). A method for the determination of phytoplankton chlorophyll and phaeophytin by fluorescence. *Deep Sea Res.* 10, 221–231.

Zubkov, M. V., and Tarran, G. A. (2008). High bacterivory by the smallest phytoplankton in the North Atlantic Ocean. *Nature* 455, 224–226. doi: 10.1038/nature07236

Zúñiga, D., Froján, M., Castro, C. G., Alonso-Pérez, F., Labarta, U., Figueiras, F. G., et al. (2013). Feedback between physiological activity of *Mytilus galloprovincialis* and biogeochemistry of the water column. *Mar. Ecol. Prog. Ser.* 476, 101–114. doi: 10.3354/meps10164